

# Global Analysis of Neutrino Oscillation

Srubabati Goswami<sup>a</sup> \* Abhijit Bandyopadhyay<sup>b</sup> and Sandhya Choubey<sup>c</sup>

<sup>a</sup> Harish-Chandra Research Institute, Chhatnag Road, Jhusi, Allahabad 211 019, INDIA

<sup>b</sup>Theory Group, Saha Institute of Nuclear Physics, 1/AF, Bidhannagar, Calcutta 700 064, INDIA

<sup>c</sup>INFN, Sezione di Trieste and Scuola Internazionale Superiore di Studi Avanzati, I-34014, Trieste, Italy

We present the constraints on neutrino oscillation parameters  $\Delta m_{\odot}^2$  and  $\theta_{\odot}$  governing the solar neutrino oscillations from two generation analysis of solar and KamLAND data. We include the latest 766.3 ton year KamLAND data in our analysis. We also present the allowed values of parameters  $\Delta m_{atm}^2$  and  $\sin^2 \theta_{atm}$  from two generation oscillation analysis of SuperKamiokande atmospheric and K2K data. For both cases we discuss the precision achieved in the present set of experiments and also how the precision can be improved in future. We also obtain the bounds on  $\theta_{13}$  from three generation analysis of global oscillation data. We emphasise on the roles played by different data sets in constraining the allowed parameter ranges.

## 1. Introduction

Compelling evidence in favour of neutrino oscillation first came from atmospheric neutrino flux measurements at SuperKamiokande (SK) [1]. The solar neutrino shortfall at SAGE, Gallex, GNO [2], Kamiokande and SK [3] were suggestive of neutrino oscillation. This was firmly established by SNO [4,5] and KamLAND (KL) [6,7]. The later provided the first evidence of oscillation of reactor neutrinos. The K2K experiment demonstrated oscillations of accelerator neutrinos [8]. Earlier the LSND [9] experiment reported positive evidence of  $\nu_{\mu}$  ( $\bar{\nu}_{\mu}$ ) oscillation using low energy accelerators though this was not confirmed by the similar experiment KARMEN. The MINIBOONE experiment will provide an independent check [10].

Aim of global oscillation analysis is to analyze the experimental data using a suitable statistical procedure and extract the information on neutrino oscillation parameters  $\Delta m^2$  (mass squared difference in vacuum) and  $\theta$  (mixing angle in vacuum). Various statistical methods have been adopted starting from the standard covariance

method, pull method [11], Frequentist method [12] and Bayesian Analysis [13].

## 2. Solar Neutrino Oscillation parameters

In this section we discuss the constraints on solar neutrino oscillation parameters  $\Delta m_{\odot}^2 \equiv \Delta m_{21}^2$ ,  $\theta_{\odot} \equiv \theta_{12}$  from two flavour  $\nu_e - \nu_{active}$  analysis.

**Allowed area from global Solar Data :** In our analysis of global solar data we include the total rates from the radiochemical experiments Cl and Ga (Gallex, SAGE and GNO combined) [2] and the 1496 day SK Zenith angle spectrum data [3], the SNO spectrum data from the pure  $D_2O$  phase [4], as well as the CC, NC and ES rates from the salt phase [5]. We use BP04 fluxes [14] and keep the  $^8B$  flux normalisation free. Further details of our analysis can be found in [15,16,17]. In the left panel of Figure 1 we show the allowed region in the parameter space including the SNO spectrum data from the pure  $D_2O$  phase while the right panel shows the allowed regions after including the data from the salt phase. The best-fit values of parameters obtained are

\*Presented the talk at Neutrino 2004

- $\Delta m_{21}^2 = 6.1 \times 10^{-5} \text{eV}^2$ ,  $\sin^2 \theta_{12} = 0.3$ ,  $f_B = 0.89$ .
  - 99% C.L. range (before salt)  
 $\Delta m_{21}^2 = (3.1-25.7) \times 10^{-5} \text{eV}^2$ ,  $\sin^2 \theta_{12} = 0.21 - 0.44$
  - 99% C.L. range (after salt)  
 $\Delta m_{21}^2 = (3.2-14.8) \times 10^{-5} \text{eV}^2$ ,  $\sin^2 \theta_{12} = 0.22 - 0.37$ .
- The allowed region corresponds to Large-Mixing-Angle (LMA) MSW solution. The impact of

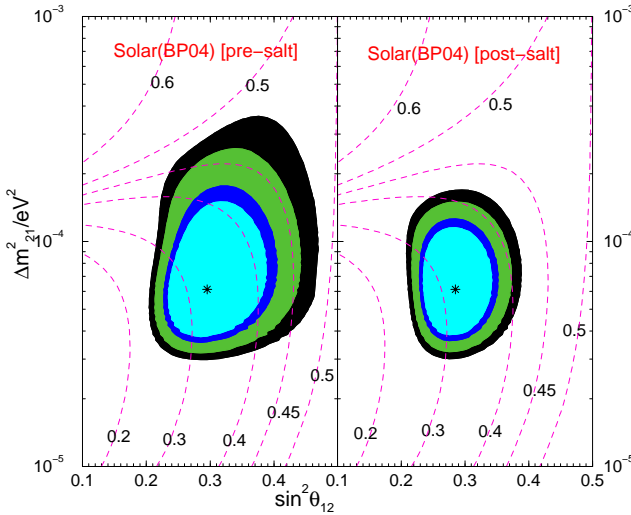


Figure 1. The 90%, 95%, 99% and 99.73% C.L. allowed regions in the  $\Delta m_{21}^2 - \sin^2 \theta_{12}$  plane from global  $\chi^2$ -analysis of solar neutrino data. Also shown are the iso-CC/NC contours.

the salt data is to tighten the upper limit on  $\Delta m_{21}^2$  and  $\sin^2 \theta_{12}$ . The iso-CC/NC curves in Fig. 1 shows that for higher values of  $\sin^2 \theta_{12}$  and  $\Delta m_{21}^2$  the CC/NC value is higher. Since the CC/NC ratio for the salt phase data is 0.31 as opposed to 0.35 in the pure  $D_2O$  phase the allowed regions shift to smaller  $\sin^2 \theta_{12}$  and  $\Delta m_{21}^2$  values following the iso-CC/NC contours.

#### Allowed area from KamLAND spectra:

We next study the impact of the new results from the KL experiment in constraining the oscillation parameters. The survival probability for

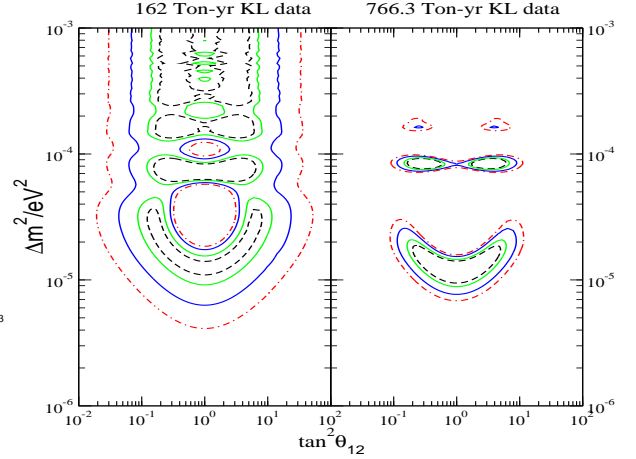


Figure 2. Same as in figure 1 but in the  $\Delta m_{21}^2 - \tan^2 \theta_{12}$  plane from global  $\chi^2$ -analysis of KL spectral data.

KL is :

$$P_{\bar{e}\bar{e}}^{KL} = 1 - \sin^2 2\theta_{12} \sin^2 \left( \frac{1.27 \Delta m_{21}^2 L}{E_\nu} \right) \quad (1)$$

neglecting the small matter effect for lower values of  $\Delta m_{21}^2$ . Assuming CPT conservation i.e same oscillation parameters for neutrinos and antineutrinos KL is sensitive to  $\Delta m_{21}^2$  in the LMA region.

In the right panel of fig 2 we show the allowed regions obtained after including the latest KL data in our analysis while the left panel shows the allowed regions without this data. The figure shows that higher  $\Delta m^2$  regions, which correspond to an averaged survival probability and hence flat spectra, reduce in size due to the increased distortion in the new KL spectrum data [7]. For details of our KL analysis we refer to [18,19].

**Allowed area from Solar+KamLAND:** In left(right) panel of 3 we present the allowed regions from analysis of solar and 162 (766.3) ton year (Ty) KL data. In the left panel there are two allowed zones – the low-LMA zone which is more favoured and the high-LMA zone admitted only at  $3\sigma$ . In the right panel there is no

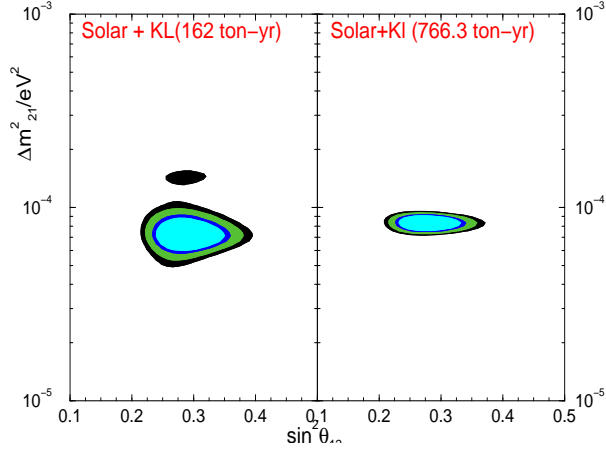


Figure 3. Same as in figure 1 but from global  $\chi^2$ -analysis of solar and KL data.

allowed high-LMA region at  $3\sigma$  since the latest KL data disfavour higher  $\Delta m_{21}^2$  values. The allowed range of  $\Delta m_{21}^2$  in low-LMA region also narrows down considerably. The best-fit points from combined analysis of solar with 162 Ty and 766.3 Ty KL data are found respectively to be

- $\Delta m_{21}^2 = 7.2 \times 10^{-5} \text{eV}^2$ ,  $\sin^2 \theta_{12} = 0.29$ ,
- $\Delta m_{21}^2 = 8.3 \times 10^{-5} \text{eV}^2$ ,  $\sin^2 \theta_{12} = 0.27$ .

The  $\theta > \pi/4$  (Dark-Side) solutions allowed by KL spectrum data get disallowed by the solar data as the matter effect in sun break the  $\theta \rightarrow \pi/2 - \theta$  symmetry (cf. fig. 5).

In fig 4 we plot  $\Delta\chi^2 = \chi^2 - \chi_{min}^2$  vs  $\Delta m_{21}^2$  (right panel) and vs.  $\sin^2 \theta_{12}$  (left panel). This figure shows that with increased statistics KL data constrains  $\Delta m_{21}^2$  more and more sharply. However  $\sin^2 \theta_{12}$  is not constrained as much. Maximal mixing is found to be more disfavoured ( $> 5\sigma$ ) by the new KL data because of increased precision.

The figure 5 shows the probabilities vs energy for KL (at an average distance of 180 km) and solar neutrinos for  $\Delta m_{21}^2 = 7 \times 10^{-5} \text{eV}^2$  and  $\sin^2 \theta_{12} = 0.3$ . For these parameters the high energy  $^8\text{B}$  solar neutrinos undergo adiabatic MSW transition with  $P_{ee} \approx \sin^2 \theta$ . For low energy solar neu-

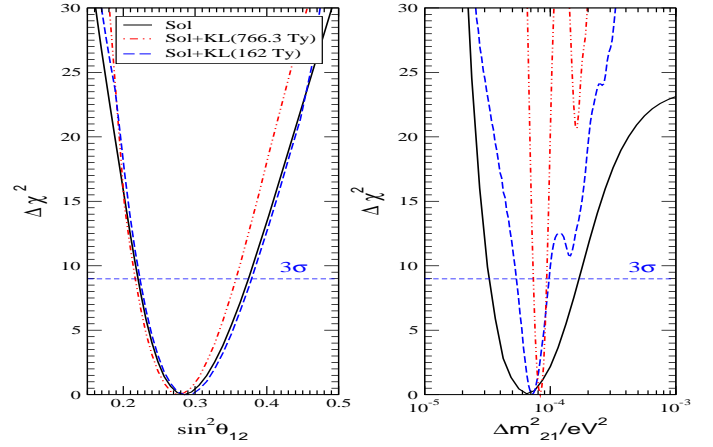


Figure 4.  $\Delta\chi^2$  vs  $\Delta m_{21}^2$  ( $\sin^2 \theta_{12}$ ) marginalised over the other parameters.

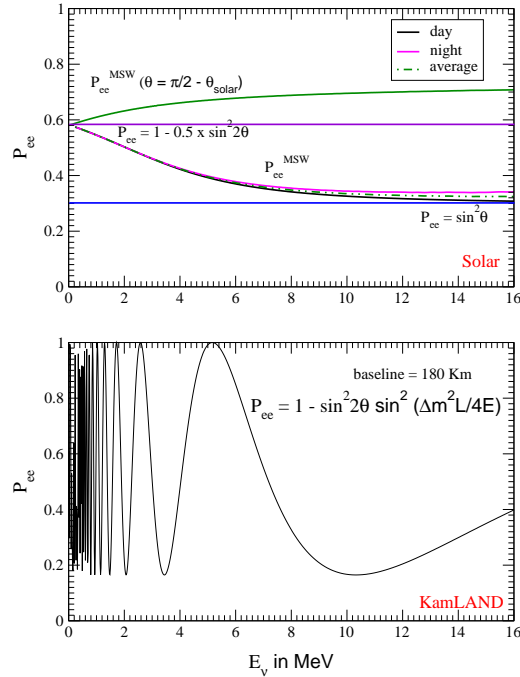


Figure 5. The probabilities for solar and KL as a function of energy

trinos  $P_{ee} \approx 1 - 0.5 \sin^2 2\theta$ . Thus with decrease in energy the survival probability increases for  $\theta < \pi/4$  causing an upturn in the observed energy spectrum. Whereas for the solar probabilities the  $\Delta m_{21}^2$  dependence is completely averaged out in KL the probability exhibits a  $L/E$  dependence which gives it an unprecedented sensitivity to  $\Delta m_{21}^2$ .

The imprint of MSW effect [20] in Sun in the solar and KL data can be quantified by parametrising the matter induced potential in the sun,  $V_{MSW} = \sqrt{2}G_F n_e$ , as  $\alpha_{MSW} \cdot V$  [21].  $\alpha_{MSW} = 0$  corresponds to no MSW effect while  $\alpha_{MSW} = 1$  corresponds to full MSW effect. Analysis performed in [21] with solar and 162 Ty KL data shows that  $\alpha_{MSW} = 0$  case is rejected at  $5.6\sigma$  w.r.t the minimum which comes at  $\alpha_{MSW} = 1$  i.e for standard MSW effect. However the allowed range of  $\alpha_{MSW}$  was found to be large. Increased statistics from KL can put stronger constraints on  $\alpha_{MSW}$  and can provide more precise test of MSW and "new" physics beyond MSW.

**Impact of each solar experiment:** In Fig. 6 we present the allowed regions obtained by taking out the data from one solar neutrino experiment from the global data set. Taking out the SNO data allows smaller values of  $f_B$ , and hence larger values of  $\sin^2 \theta_{12}$  ( $P_{ee} \sim f_B \sin^2 \theta_{12}$ ). With 162 Ty KL data excluding SNO allowed maximal mixing, Dark side and higher  $\Delta m^2$  solutions. With the spectral distortion observed in the 766.3 Ty KL data these regions are ruled out with increased confidence even without SNO.

**On the precision of  $\nu_\odot$  oscillation parameters:**

In Table 1 we present the  $3\sigma$  allowed ranges of  $\Delta m_{21}^2$  and  $\sin^2 \theta_{12}$ , obtained using different data sets. We also show the uncertainty in the value of the parameters through a quantity "spread" which we define in general as

$$\text{spread} = \frac{\Delta m^2(\sin^2 \theta)_{max} - \Delta m^2(\sin^2 \theta)_{min}}{\Delta m^2(\sin^2 \theta)_{max} + \Delta m^2(\sin^2 \theta)_{min}} \quad (2)$$

Table 1 illustrates the remarkable sensitivity of KL in reducing the uncertainty in  $\Delta m_{21}^2$ . But  $\theta_{12}$  is not constrained much better than the current

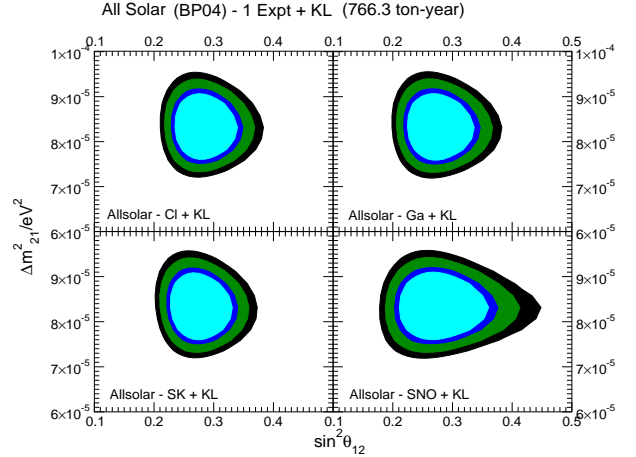


Figure 6. The allowed regions in  $\Delta m_{21}^2$  -  $\sin^2 \theta_{12}$  plane, obtained by removing the data from one solar neutrino experiment from the global fit. These figures are drawn on a linear scale for  $\Delta m_{21}^2$ .

set of solar experiments. The reason for this is the average energy and distance in KL corresponds to a Survival Probability MAXimum (SPMAX) i.e  $\sin^2(\Delta m_{21}^2 L/4E) \approx 0$ . This means that the coefficient of the  $\sin^2 2\theta_{12}$  term in  $P_{ee}^{KL}$  is relatively small, weakening the sensitivity of KL to  $\theta_{12}$ . The precision in  $\theta_{12}$  can be improved by reducing the baseline length such that one gets a minimum of the  $\bar{\nu}_e$  survival probability (SPMIN) where  $\sin^2(\Delta m_{21}^2 L/4E) = 1$ . This corresponds to a distance  $L = 1.24(E/MeV)(eV^2/\Delta m_{12}^2)$  m. For the low-LMA solution region and the average energy of neutrinos in KL experiment, this corresponds to a distance of approximately (50 - 70) km [23]. For an experiment with a 70 km baseline and 24.3 GW reactor power  $\sin^2 \theta_{12}$  can be determined with  $\sim 10\%$  error at 99% C.L. with a 3 kTy statistics [23].

Improved sensitivity in the measurement of  $\theta_{12}$  is possible from LowNu experiments [22]. The pp flux is known with 1% accuracy from Standard Solar Models as compared to the uncertainties of  ${}^8B \sim 20\%$  and  ${}^7Be \sim 10\%$ . At the low energies relevant for pp neutrinos  $P_{ee} \approx 1 - \frac{1}{2} \sin^2 2\theta$  re-

Table 1

$3\sigma$  allowed ranges and % spread of  $\Delta m_{21}^2$  and  $\sin^2 \theta_{12}$  obtained from 2 parameter plots.

Data set used	( $3\sigma$ )Range of $\Delta m_{21}^2$ eV <sup>2</sup>	( $3\sigma$ )spread in $\Delta m_{21}^2$	( $3\sigma$ ) Range of $\sin^2 \theta_{12}$	( $3\sigma$ ) spread in $\sin^2 \theta_{12}$
only sol	3.0 - 17.0	70%	0.21 - 0.39	30%
sol+162 Ty KL	4.9 - 10.7	37%	0.21 - 0.39	30%
sol+ 766.3 Ty KL	7.2 - 9.5	14%	0.21 - 0.37	27%

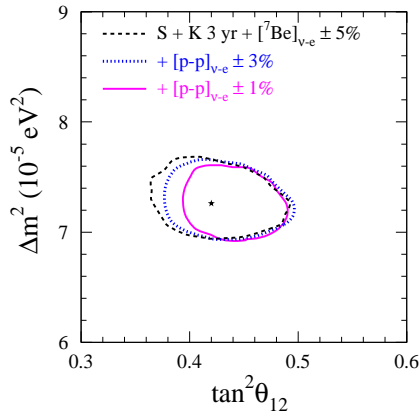


Figure 7. Allowed area including the rates from a generic pp neutrino experiment with different errors. Figure taken from [24]

sulting in a heightened sensitivity to  $\theta_{12}$ . In 7 we show the allowed region [24] in  $\Delta m^2 - \tan^2 \theta_{12}$  plane including fictitious results from a generic pp scattering experiment. The figure shows that precision in  $\theta_{12}$  increases with reduced error in pp flux measurement.

The recently proposed Gd loaded SK detector can measure  $\Delta m_{21}^2$  with  $\sim 1\%$  and  $\sin^2 \theta_{12}$  with  $\sim 15\%$  uncertainty at 99% C.L. after 5 years of data taking [25].

### 3. Atmospheric Neutrino Oscillation Parameters

In this section we present the constraints on atmospheric neutrino oscillation parameters  $\Delta m_{32}^2 \equiv \Delta m_{atm}^2$  and  $\sin^2 \theta_{23} \equiv \sin^2 \theta_{atm}$  from

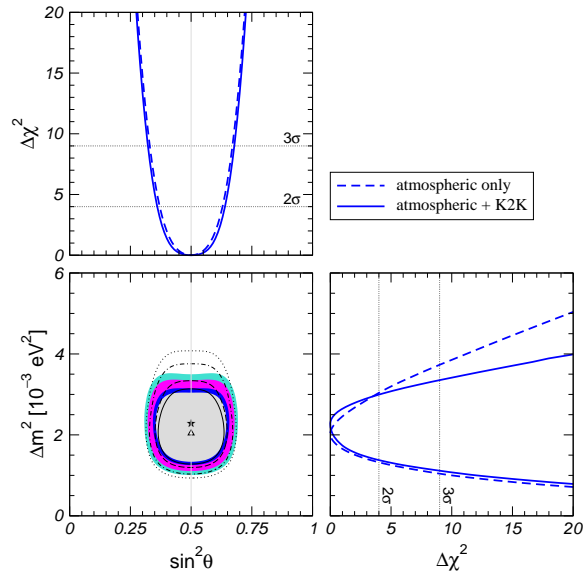


Figure 8. The allowed regions from SK (line contours) and SK+K2K (shaded contours) analysis from a two flavour analysis. Also shown is the  $\Delta\chi^2$  vs  $\Delta m_{atm}^2$  and  $\sin^2 \theta_{atm}$  marginalised w.r.t the undisplayed parameter[28]

two flavour oscillation analysis SK and SK+K2K data.

#### Allowed parameters from SK+K2K analysis:

In 2003 the SK collaboration reanalyzed their data and reported a downward shift of the allowed  $\Delta m_{atm}^2$  from a two-generation analysis due to incorporation of three-dimensional Honda atmospheric fluxes and revised cross-section and

efficiencies. The best-fit value of  $\Delta m_{atm}^2$  from SK zenith angle data reported in this conference is  $2.1 \times 10^{-3} \text{ eV}^2$  [26]. Analysis of SuperKamiokande data by two groups confirm this downward shift of  $\Delta m_{atm}^2$  [27,28].

The K2K experiment which is sensitive to atmospheric neutrino oscillation parameters gives the best-fit as  $\Delta m_{atm}^2 = 2.8 \times 10^{-3} \text{ eV}^2$   $\sin^2 2\theta_{atm} = 1.0$ .

In fig. 8 we show the allowed regions in  $\Delta m_{atm}^2$  -  $\sin^2 \theta_{atm}$  plane from analysis of SK data as well as from combined analysis of SK+K2K data [28]. The best-fit from the combined analysis corresponds to

- $\Delta m_{atm}^2 = 2.3 \times 10^{-3} \text{ eV}^2$ ,  $\sin^2 \theta_{atm} = 0.5$ .
- Higher  $\Delta m^2$  values are seen to be constrained by K2K but  $\theta_{atm}$  is not constrained any better. For a two generation analysis the relevant probability for both SK and K2K are vacuum oscillation probability and the allowed regions are symmetric about  $\theta_{23}$  and  $\pi/2 - \theta_{23}$ .

Recently SuperKamiokande has reported the observation of the first oscillation minima in the  $L/E$  distribution [29]. The observation of this first dip disfavors the neutrino decay and de-coherence solutions. The best-fit value of  $\Delta m_{atm}^2$  from this analysis is  $2.4 \times 10^{-3} \text{ eV}^2$  with  $\sin^2 2\theta_{atm} = 1.0$ . The allowed ranges of parameters from the two different analyses are:

- 90% C.L. range (SK L/E)  
 $\Delta m_{atm}^2 = 1.9 - 3.0 \times 10^{-3} \text{ eV}^2$ ,  $\sin^2 2\theta_{atm} > 0.9$
- 90% C.L. range (SK Zenith)  
 $\Delta m_{atm}^2 = 1.3 - 3.0 \times 10^{-3} \text{ eV}^2$ ,  $\sin^2 2\theta_{atm} > 0.9$

#### Precision of atmospheric neutrino oscillation parameters:

The spread in  $\Delta m_{atm}^2$  is 39% from SK zenith data whereas it is 22% from SK L/E data. Thus improved precision in  $\Delta m_{atm}^2$  is obtained with L/E data. Range of  $\sin^2 \theta_{atm}$  however remains unchanged:  $\delta(\sin^2 2\theta_{23}) \sim 5\%$ . However  $\delta(\sin^2 \theta_{23}) \sim 32\%$  because  $\sin^2 \theta_{23}$  precision is worse than  $\sin^2 2\theta_{23}$  precision near maximal mixing. Increased statistics in  $L/E$  data can improve  $\Delta m_{32}^2$  uncertainty to  $\sim 10\%$  at 90% C.L. in 20 years of operation of SK [30]. This is sensitive to the true  $\Delta m_{32}^2$  chosen and the above precision is achieved for  $\Delta m_{32}^2 = 2.5 \times 10^{-3}$

$\text{eV}^2$ . But precision in  $\sin^2 \theta_{23}$  does not improve with increased statistics [30]. Large Magnetized Iron calorimeters for atmospheric neutrinos (e.g MONOLITH,INO) [31,32] can improve the precision in both atmospheric parameters.

#### 4. Three Flavour Oscillation

The oscillation parameters for a three flavour analysis are two mass squared differences  $\Delta m_{31}^2 = \Delta m_{\odot}^2$ ,  $\Delta m_{31}^2 = \Delta m_{CHOOZ}^2 \simeq \Delta m_{atm}^2 = \Delta m_{32}^2$  and three mixing angles which are usually denoted as  $\theta_{12}, \theta_{23}$  and  $\theta_{13}$  with the mixing matrix  $U$  parameterized in the standard MNS form. In the limit  $\Delta m_{21}^2 \ll \Delta m_{32}^2$  as is indicated by the two generation analysis of atmospheric and solar neutrino data. In this limit the atmospheric probabilities depend on  $\Delta m_{32}^2$ ,  $\theta_{13}$ ,  $\theta_{23}$  and solar neutrino probabilities depend on  $\Delta m_{21}^2$ ,  $\theta_{12}$ ,  $\theta_{13}$ . The CP violation phases can be neglected in this limit. Clearly for  $\theta_{13} = 0$  solar and atmospheric neutrinos decouple. The probability for the CHOOZ reactor experiment depends on  $\Delta m_{31}^2$  and  $\theta_{13}$ .

**Bound on  $\sin^2 \theta_{13}$ :** CHOOZ/PaloVerde experiment has put stringent bounds on  $\theta_{13}$  from non-observation of  $\bar{\nu}_e$  disappearance [33]. In fig 9 we show the allowed area from CHOOZ experiment in  $\Delta m_{31}^2 - \tan^2 \theta_{13}$  plane. The area shaded by vertical blue (slanting red) lines correspond to the allowed range of  $\Delta m_{31}^2$  from two generation analysis of SK L/E (zenith) + K2K atmospheric neutrino data [34,35]. The figure shows that the  $\theta_{13}$  bound from CHOOZ depends sensitively on  $\Delta m_{31}^2$ . Stronger bounds are obtained for higher  $\Delta m_{31}^2$ .

In figure 10 we show the limits on  $\theta_{13}$  obtained from  $\Delta\chi^2$  vs  $\theta_{13}$  plots. We marginalise over all other parameters. We let  $\Delta m_{31}^2$  vary freely within the  $3\sigma$  range obtained using the one parameter  $\Delta\chi^2$  vs  $\Delta m_{31}^2$  fit as given in the latest SK analysis [26]. The bounds that we get are

- $\sin^2 \theta_{13} < 0.071$  (CHOOZ+atm)
- $\sin^2 \theta_{13} < 0.063$  (sol+KL (162)+CHOOZ+atm)<sup>2</sup>
- $\sin^2 \theta_{13} < 0.05$  (sol+KL (766.3)+CHOOZ+atm)

<sup>2</sup>Using the range of  $\Delta m_{31}^2$  from the SK+K2K analysis of [34] bound comes as  $\sin^2 \theta_{13} < 0.077$  [17]

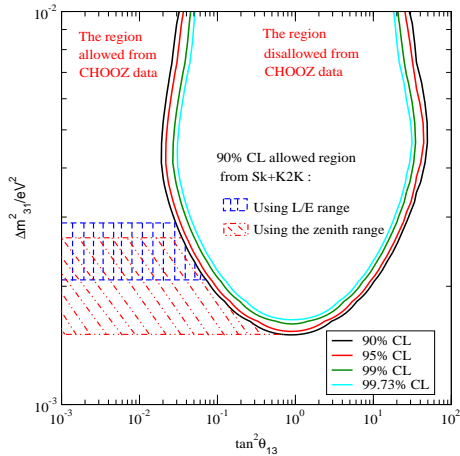


Figure 9. Allowed area in  $\Delta m_{31}^2 - \tan^2 \theta_{13}$  plane from CHOOZ data. The shaded regions correspond to the allowed range of  $\Delta m_{31}^2$  using SK zenith angle (L/E) and K2K data [34,35].

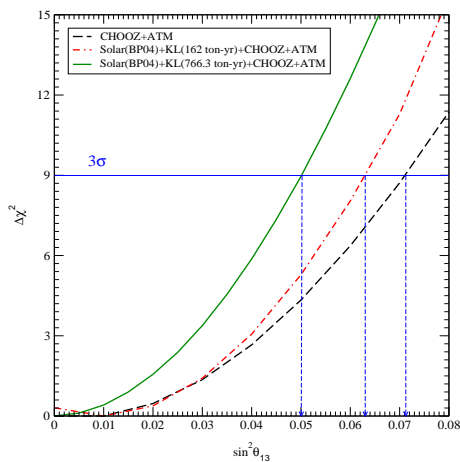


Figure 10. Bounds on the mixing angle  $\theta_{13}$  from data combination. Also shown is the  $3\sigma \Delta\chi^2$  limit for 1 parameter.

A non-zero  $\theta_{13}$  prefers higher  $\Delta m_{21}^2$  values which is disfavoured by the solar+KL data. Because of this the combined  $\chi^2$  increases making the bound on  $\theta_{13}$  stronger than compared to only CHOOZ+atmospheric. Since the recent KL data disfavours high  $\Delta m_{21}^2$  values to a greater extent the bound on  $\theta_{13}$  further improves by including it.

In 11 we show the effect of non-zero  $\sin^2 \theta_{13}$  on the allowed area in solar neutrino parameter space. The presence of a small non-zero  $\theta_{13}$  can improve the fit in the regions of the parameter space with higher values of  $\Delta m_{21}^2$  [17], i.e., in the high-LMA zone. But due to increased discord between the new KL data and high  $\Delta m_{21}^2$  values the high-LMA region now gets excluded at more than  $3\sigma$  even in the presence of a third generation in the mixing, indicating the robustness of the low-LMA solution. The allowed atmospheric regions in  $\Delta m_{31}^2 - \sin^2 2\theta_{23}$  plane also remains stable in presence of non-zero  $\theta_{13}$  [28]. Including the  $\Delta m_{21}^2$  terms in the analysis one can give bound on the hierarchy parameter  $\alpha = \Delta m_{21}^2 / \Delta m_{31}^2$  associated with subleading oscillations for atmospheric neutrinos as well as for long baseline studies. The best-fit for this comes as  $\alpha = 0.03$  [28].

## 5. Conclusions

A series of seminal experiments performed over a period of nearly four decades and more and more refined analysis of the global experimental data has not only confirmed the existence of neutrino mass and mixing, but also narrowed down the allowed parameter ranges considerably heralding the precision era in neutrino physics.

The prime future goals for neutrino oscillation studies are- further improvement of precision of the parameters, to obtain some measure of smallness of  $\theta_{13}$ , to determine the sign of  $\Delta m_{32}^2$  and to search for CP violation in the lepton sector.

**Acknowledgements:** S.G. would like to thank the organizers of Neutrino 2004 for the invitation to give this talk and T. Kajita, E. Lisi and M. Maltoni for many helpful discussions during the preparation of the talk.

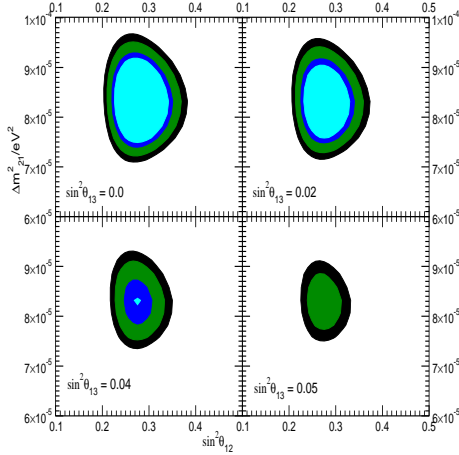


Figure 11. Same as in figure 1 but from a three flavour analysis of the global solar and reactor neutrino data and plotted on a linear scale for  $\Delta m_{21}^2$ .

## REFERENCES

1. Y. Fukuda *et al.* Phys. Rev. Lett. **81**, 1562 (1998).
2. B. T. Cleveland *et al.*, Astrophys. J. **496**, 505 (1998); J. N. Abdurashitov *et al.* astro-ph/0204245; W. Hampel *et al.* Phys. Lett. B **447**, 127 (1999); C.M. Cattadori, Nucl. Phys. **B110**, Proc. Suppl, 311 (2002).
3. S. Fukuda *et al.* Phys. Lett. B **539**, 179 (2002).
4. Q. R. Ahmad *et al.* Phys. Rev. Lett. **89**, 011301 (2002). *ibid.*, 011302 (2002).
5. S. N. Ahmed *et al.* nucl-ex/0309004.
6. K. Eguchi *et al.*, Phys. Rev. Lett. **90**, 021802 (2003).
7. G. Gratta, talk at Neutrino 2004; T. Araki *et al.*, hep-ex/0406035.
8. T. Nakaya, talk at Neutrino 2004.
9. C. Athanassopoulos *et al.*, Phys. Rev. Lett. **77**, 3082 (1996); *ibid.* **81**, 1774 (1998).
10. S. Brice, talk at Neutrino 2004.
11. G. L. Fogli *et al.*, Phys. Rev. D **66**, 053010 (2002).
12. P. Creminelli, G. Signorelli and A. Strumia,

JHEP **0105**, 052 (2001).

13. M. V. Garzelli and C. Giunti, JHEP **0112**, 017 (2001).
14. J. N. Bahcall and M. H. Pinsonneault, Phys. Rev. Lett. **92**, 121301 (2004).
15. A. Bandyopadhyay, *et al.*, Phys. Lett. B **519**, 83 (2001).
16. A. Bandyopadhyay *et al.*, Phys. Lett. B **540**, 14 (2002); S. Choubey *et al.* hep-ph/0209222.
17. A. Bandyopadhyay *et al.*, hep-ph/0309174.
18. A. Bandyopadhyay *et al.*, hep-ph/0406328.
19. A. Bandyopadhyay *et al.*, Phys. Lett. B **559**, 121 (2003); J. Phys. G **29**, 2465 (2003).
20. L. Wolfenstein, Phys. Rev. D **17**, 2369 (1978); S. P. Mikheev and A. Y. Smirnov, Sov. J. Nucl. Phys. **42** (1985) 913 [Yad. Fiz. **42**, 1441 (1985)].
21. G. L. Fogli *et al.*, Phys. Lett. B **583**, 149 (2004).
22. See for e.g. the talk by Y. Suzuki, Neutrino 2004.
23. A. Bandyopadhyay, S. Choubey and S. Goswami, Phys. Rev. D **67**, 113011 (2003).
24. J. N. Bahcall and C. Pena-Garay, JHEP **0311**, 004 (2003).
25. J. F. Beacom and M. R. Vagins, hep-ph/0309300. S. Choubey and S. T. Petcov, hep-ph/0404103.
26. E. Kearns, talk at Neutrino 2004, Paris.
27. M. C. Gonzalez-Garcia and M. Maltoni, hep-ph/0406056.
28. M. Maltoni *et al.*, hep-ph/0405172.
29. Y. Ashie *et al.*, hep-ex/0404034.
30. T. Kajita, Talk at NOON04.
31. N.Y. Agafonova *et al.*, LNGS-P26-2000; <http://castore.mi.infn.it/~monolith/>
32. See <http://www.imsc.res.in/~ino>.
33. M. Apollonio *et al.*, Phys. Lett. **B466** (1999) 415; F. Boehm *et al.*, Phys. Rev. Lett. **84** (2000) 3764.
34. The  $\Delta m_{31}^2$  range from SK zenith +K2K analysis is taken from G. L. Fogli *et al.* Phys. Rev. D **69**, 017301 (2004).
35. The  $\Delta m_{31}^2$  range from SK L/E +K2K analysis is provided by G. L. Fogli, E. Lisi, A. Marrone, A. Palazzo in a private communication.